Non-equilibrium Self-Assembly

DOI: 10.1002/ange.201301386

The Rate of Energy Dissipation Determines Probabilities of Non-equilibrium Assemblies**

*Konstantin V. Tretiakov, Igal Szleifer, and Bartosz A. Grzybowski**

Beyond construction of ordered, equilibrium structures, one of the grand visions of self-assembly research is to organize matter away from thermodynamic equilibrium.[1] The inspiration for such dynamic/non-equilibrium self-assembly,[2] NESA, comes largely from biology[2c,d] (with cells and organisms being perfect examples of non-equilibrium assemblies), while its promise lies in the new types of dynamic materials[3a–d] and chemical systems[3e–g] that could harness and dissipate the externally delivered energy to sense and adapt to the environment, reconfigure, exhibit taxis, or even self-replicate. Despite recent progress,[2,3] however, NESA remains an experimental challenge and is also in need of unifying statistical–thermodynamic principles. At equilibrium, the Boltzmann relation $P(E) \propto \exp(-E/kT)$ provides a powerful and predictive link between the probability P of structure formation and its energy E. In the non-equilibrium (NE) regime, such general principles do not exist, and our understanding of NE thermodynamics is largely limited to the so-called near-equilibrium conditions.[4] There, the formalism developed by Prigogine some seven decades ago[4c] prescribes that the structures that are formed minimize the entropy production dS/dt and the rate ε at which energy is dissipated (see Methods). Although the validity of this minimal entropy production (MEP) rule has been questioned,[5] and Prigogine himself clearly emphasized that it applies only "sufficiently close to equilibrium," his Nobel Prizewinning work has subsequently assumed life of its own, with frequent interpretations[6] suggesting that Nature generally forms minimally dissipative structures and systems. Indeed, does it? To answer this question requires a rigorous approach. First, a NE system must be implemented that has a "choice" of evolving into more than one dissipative structure. Second, these possible structures should differ only in their rates of energy dissipation, and not in energies or other parameters; if many parameters differed simultaneously, it would be impossible to attribute the formation of a given structure to the dissipation rate alone. Third, it should be possible to quantify the frequencies with which different structures form. Upon normalization of these frequencies, one could then calculate occurrence probabilities and finally relate them to the energy dissipation rates, $P = f(\varepsilon)$.

This is precisely what we set out to accomplish in the present work. We describe a NESA system that can evolve, for the same system parameters, into two distinct dynamic "polymorphs", for which the probabilities of occurrence depend only on the dissipation rates. Combining experiment and theory, we then show that NESA can produce both low- and high-dissipation structures. Moreover, based on several thousand self-assembly experiments, we collect robust statistics according to which probabilities of observing low/high dissipation assemblies change with the difference in their dissipation rates: specifically, when the dissipation "gap" $\Delta\varepsilon$ between the possible assemblies increases, the less-dissipative structure becomes exponentially more likely. Interestingly, the equations we derive converge onto MEP only in the limit when one state is infinitely less dissipative than the other (that is, when $\Delta\varepsilon \to \infty$), and the low-dissipation structure alone is observed. Overall, to the best of our knowledge, our results demonstrate for the first time that while nature prefers less dissipative assemblies, it also allows thermodynamically more wasteful structures to form spontaneously, albeit with exponentially decreasing probabilities.

The first consideration is the choice of the system. Although a molecular-scale study would be desirable, no molecules or nanoobjects are yet known to self-assemble into multiple dissipative structures. Furthermore, the currently available methods (either experimental or theoretical) do not allow for accurate determination of entropy production and the rate of energy dissipation in molecular systems (that is, what fraction of an external energy input is used to set up dissipative interactions between the molecules and what fraction goes into other degrees of freedom, for example solvent). This limitation is not present in fluidic systems, in which the solution to the Navier–Stokes equations of fluid motion yields the so-called viscous dissipation function Φ and the energy dissipation rate ε (and thus dS/dt; see Methods). Accordingly, the system we use is based on fluidic interactions.

This system is illustrated in Figure 1 and comprises millimeter-sized polymeric particles loaded with 5–30% magnetite and placed at an interface between air and liquid (here, various mixtures of diethylene glycol, EG_2, and water) and subject to a magnetic field produced by a rotating permanent magnet ($5.6 \times 4 \times 1\ cm^3$, magnetization ca.

[*] Prof. I. Szleifer, Prof. B. A. Grzybowski
Department of Chemistry, Northwestern University
2145 Sheridan Road, Evanston, IL 60208 (USA)
E-mail: grzybor@northwestern.edu
Homepage: http://dysa.northwestern.edu
Dr. K. V. Tretiakov
Institute of Molecular Physics, Polish Academy of Sciences
M. Smoluchowskiego 17/19, 60-179 Poznań (Poland)

[**] This work was supported by the Non-equilibrium Energy Research Center (NERC), which is an Energy Frontier Research Center funded by the U.S. Department of Energy, Office of Science, Office of Basic Energy Sciences under Award Number DE-SC0000989. The authors are grateful to the Poznań Supercomputing Center (PCSS) in Poland for supporting thousands of hours of supercomputer time.

Supporting information for this article is available on the WWW under http://dx.doi.org/10.1002/anie.201301386.

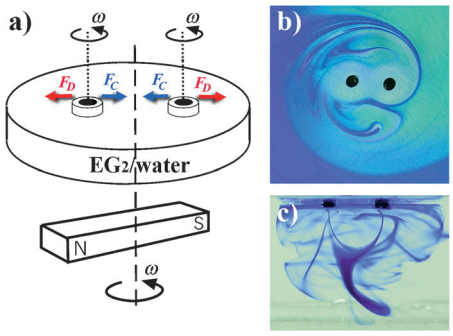

Figure 1. a) The experimental arrangement, in which an external magnet drives the rotations of small magnetic particles immersed in a viscous liquid at a liquid–air interface. Repulsive vortex–vortex forces are indicated by red arrows; the confining magnetic forces are indicated by blue arrows. b) Top view of the flows around two rotating particles (each 2 mm in diameter) visualized by the addition of dye (Crystal Violet). c) The corresponding side view (that is, a view along the plane of the interface).

1000 G cm^{-3}; for further technical details, see Ref. [7a,b]). In the absence of the external field, the particles are randomly distributed over the interface and are stationary. When the field is turned on, however, the particles start rotating (with typical angular velocity $\omega \approx 10$ Hz, equal to that of the magnet) and create vortices in the surrounding fluid. These vortices translate into repulsive interactions between the particles (F_D in Figure 1a). At the same time, the rotating magnet gives rise to a confining magnetic potential and all particles experience a centrosymmetric force F_C that attracts them toward the axis of rotation of the magnet. Importantly, in the regime of Reynolds numbers[8] Re ≈ 1, the competition between F_C and F_D evolves particles into open-lattice "crystals"[7] such as those shown in Figure 1b and Figure 2 (see also the Movies in the Supporting Information). These non-equilibrium assemblies persist only as long as the particles harness energy from the external rotating magnetic field and then dissipate this "captured" energy into fluid flows.

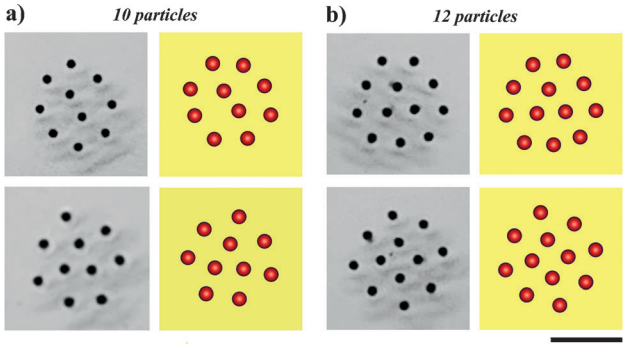

Figure 2. Polymorphic structures observed for a) $n = 10$ and b) $n = 12$ rotating particles in experiments (monochrome images) and in the simulations (color images). The particular experimental structures were obtained at $\omega = 500$ rpm in a 3:1 w/w mixture of diethylene glycol and water (Re ≈ 0.52 based on the viscosity data from Ref. [9]). Scale bar (for all experimental images): 1 cm.

For most particle numbers n, the assemblies that form are morphologically unique;[7a,b] for $n = 10$ and $n = 12$, however, the initially randomly placed particles can evolve into two distinct and stable configurations (Figure 2). For $n = 10$ (Figure 2a), one structure that forms has two particles in the inner shell, and the other, three; we denote these configurations {10,2} and {10,3}, respectively. For $n = 12$ (Figure 2b), the two stable polymorphs are {12,3} and {12,4}. In experiments, all of these structures are stable for days, provided that the Reynolds numbers are between about 0.3–0.65; the intuitive meaning of Re in our experiments is that this parameter (adjustable by the viscosity or rotational speeds of the fluid[8]) controls the strengths of vortex–vortex repulsions, and thus the sizes,[7] energies, and dissipation rates of our dynamic crystals.

To analyze the $n = 10$ and $n = 12$ polymorphs, we first performed a series of experiments in which the particles were started from random initial configurations at the interface at least 200 times for each value of Re (see the Movies in the Supporting Information). In this way, we were able to estimate experimental probabilities with which each of the possible structures/polymorphs is realized under given conditions. Figure 3a,b summarizes the results. For $n = 10$, the {10,2} state is more probable than {10,3} (that is, $P_{\{10,2\}} > P_{\{10,3\}}$), although its probability decreases with increasing Re. For $n =$

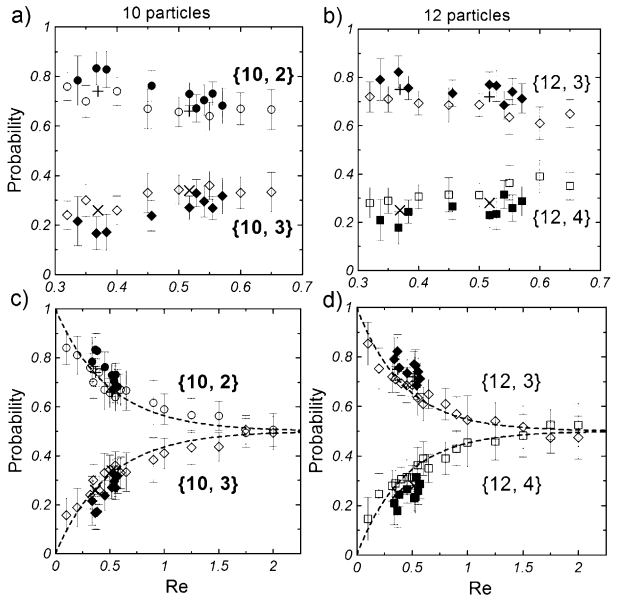

Figure 3. Statistics of non-equilibrium, dissipative assemblies. The plots have the probabilities of structure occurrence P as a function of the Reynolds number for a),c) $n = 10$ and b),d) $n = 12$ rotating particles. Filled symbols: experimental data; open symbols: simulations. a),b) Data for the range of Re values that can be realized in experiments; c),d) results plotted over the entire range of Re values that give stable structures in the simulations. In both experiments and simulations, standard deviations are based on at least 200 independent experiments/simulation runs for each condition. Lines in (c) and (d) are fits to the functions of the form $P(\mathrm{Re}) = (1 \pm \exp(-a_n \mathrm{Re}))/2$ ($a_{10} = 2.0621$, $a_{12} = 2.3456$). In experiments, the temperature was kept constant at 27 °C and Re values were varied by changing the composition of the diethylene glycol/water mixture.[9]

12, the {12,3} state is realized more often than {12,4} (that is, $P_{\{12,3\}} > P_{\{12,4\}}$), with $P_{\{12,3\}}$ decreasing with decreasing Re.

These experimental studies provide a benchmark for the computer simulations we consider next. The underlying reasoning is that if the simulations reproduce the experimental occurrence probabilities, the computational method is accurate and can reliably calculate the dissipation rates ε (which, as mentioned above, cannot be determined directly from experiments). In this way, we will ultimately be able to relate $P(\varepsilon)$ to ε.

The computational approach, which was originally developed and validated by Maxey and Karniadakis, has been described in detail.[7c] Solving the Navier–Stokes (NS) equations of fluid motion permits for the calculation of the viscous stress tensor and the hydrodynamic interactions between the rotating particles. Taking into account the conservative forces that are due to the field of the rotating magnet then leads to the equations describing motions of the particles in the fluid (for details, see Methods). When implemented, the above method reproduces the experimental dynamics of the particles faithfully. Repeating the simulation several hundred times for each value of Re and with different initial configurations of particles (more than 5000 hours of supercomputer time in total) yields the statistics of "polymorphic" structures that are close (to within 10%) to the experimental results for both $n=10$ and $n=12$ (open symbols in Figure 3a,b). The calculations based on ideally shaped rotors and without any disturbances seen in experiments[8] allow the system dynamics to be studied over a wider range of Re values of up to about 2. The results of these calculations are summarized in Figure 3c and d: importantly, the probabilities of occurrence scale as $P(\mathrm{Re}) = (1 \pm \exp(-a_n \mathrm{Re}))/2$ (dashed lines in Figure 3c,d).

Having calibrated the simulations against experiments, the key challenge is then to relate the observed/calculated probabilities of occurrence of polymorphs to their energies and/or energy dissipation rates. To this end, for every value of Re and every polymorph $\{n,k\}$, we calculated (see Methods) the kinetic energies that are due to particle translations $K_{\{n,k\}}$, potential energies that are due to the confinement in the magnetic field $U_{\{n,k\}}$, kinetic energies of the fluid $K^f_{\{n,k\}}$, total energies $E_{\{n,k\}} = K_{\{n,k\}} + U_{\{n,k\}} + K^f_{\{n,k\}}$, and the viscous energy dissipation rates ε. These rates quantify the fraction of energy that the magnetic rotors harness from the external rotating magnetic field and then dissipate into fluid flows to maintain ordered particle assemblies. For a given flow field and configuration of rotating particles, ε is calculated by integrating the viscous dissipation function Φ over the entire simulation domain (see Methods and the Supporting Information).

Figure 4a,b plots the non-dimensionalized differences Δ in these quantities between the polymorphs (with the convention of the lower k polymorph being subtracted: for example, for $n=10$, $\Delta E_{10} = E_{\{10,3\}} - E_{\{10,2\}}$, $\Delta\varepsilon_{10} = \varepsilon_{\{10,3\}} - \varepsilon_{\{10,2\}}$, and so on). Remarkably, over the entire range of Re values studied, the energy differences are constant to a very good approximation and their variability is much smaller than the changes in the differences of the dissipation rates $\Delta\varepsilon$. Moreover, as illustrated in the Supporting Information, Figure S1, the ratios $\omega\Delta E_n/\Delta\varepsilon_n$ scale linearly with Re.

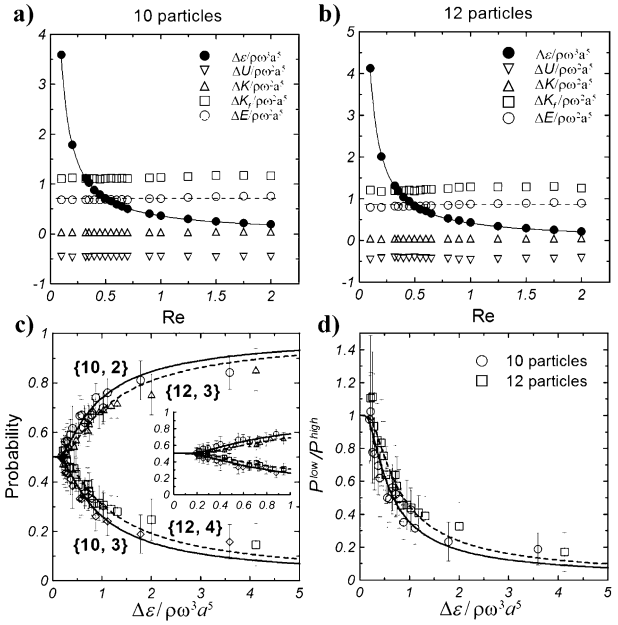

Figure 4. The dissipation rate, which determines the emergence of dissipative structures. a),b) Differences in the calculated, non-dimensionalized energy dissipation rates $\Delta\varepsilon$, potential energies ΔU, kinetic energies of the particles ΔK, kinetic energies of the fluid ΔK^f, and total energies ΔE plotted as a function of Re for systems of 10 and 12 particles. The values of $\Delta\varepsilon$ (solid symbols) change strongly and scale inversely with Re; the fits to the data are $\Delta\varepsilon_{10}/\rho\omega^3a^5 = 0.3584/\mathrm{Re}$ ($R^2 = 0.999882$) and $\Delta\varepsilon_{12}/\rho\omega^3a^5 = 0.4127/\mathrm{Re}$ ($R^2 = 0.999473$). In sharp contrast, the energy differences (open symbols) for each polymorph do not change perceptibly over the entire range of Re values. Dashed lines trace the non-dimensionalized total energies $\omega\langle\Delta E_{10}\rangle_{\mathrm{Re}}/\rho\omega^3a^5 = 0.7117$ and $\omega\langle\Delta E_{12}\rangle_{\mathrm{Re}}/\rho\omega^3a^5 = 0.85$ (Supporting Information, Figure S1). c) Probabilities of occurrence of various polymorphs plotted as a function of the calculated values of $\Delta\varepsilon$. Symbols are based on data from Figure 3. Lines are based on Equations (1) and (2) in the text. d) Ratios of probabilities of the less-likely/more-dissipative (P^{low}) to the more-likely/less-dissipative (P^{high}) structures for $n=10$ and $n=12$.

Combining these results with the P versus Re dependencies from Figure 3, the probabilities of assemblies can be written as functions of $\Delta\varepsilon$:

$$P_n^{\mathrm{high}} = (1 + \exp(-C_n/\Delta\varepsilon_n))/2 \quad (1)$$

$$P_n^{\mathrm{low}} = (1 - \exp(-C_n/\Delta\varepsilon_n))/2 \quad (2)$$

with fitting constants $C_{10} = 0.739\rho\omega^3a^5$ and $C_{12} = 0.968\rho\omega^3a^5$, and subscripts high and low denoting states observed with higher and lower probabilities, respectively (see Figure 3). Alternatively, we can express the ratio of probabilities (Figure 4c,d) as:

$$\frac{P_n^{\mathrm{low}}}{P_n^{\mathrm{high}}} = 1 - \frac{2}{1 + \exp(C_n/\Delta\varepsilon_n)} \quad (3)$$

The above equations are the key result of our work and can be interpreted as follows: 1) For a system in which the components can evolve/assemble into multiple stable NE

structures, the less dissipative structures have higher probability of occurrence. In our system, for $n=10$, $\varepsilon_{\{10,2\}}<\varepsilon_{\{10,3\}}$, and $P_{\{10,2\}}>P_{\{10,3\}}$, while for $n=12$, $\varepsilon_{\{12,3\}}<\varepsilon_{\{12,4\}}$, and $P_{\{12,3\}}>P_{\{12,4\}}$; 2) As the dissipation "gap" $\Delta\varepsilon$ increases, the less dissipative structures (here, {10,2} and {12,3}) become exponentially more likely; 3) In the limit when the difference in the dissipation rates of the possible stable structures becomes infinite, the probability of the low-dissipation structure tends to unity and that of the high-dissipation structure tends to zero (that is, when $\Delta\varepsilon\rightarrow\infty$, $P^{\text{high}}=1$ and $P^{\text{low}}=0$); 4) In the limit when the dissipation rates of the available structures are equal, their probabilities of occurrence are also equal (that is, when $\Delta\varepsilon\rightarrow 0$, $P^{\text{high}}=1/2$ and $P^{\text{low}}=1/2$).

It is instructive to compare the above results with the MEP principle of Prigogine, which stipulates that NE systems close to equilibrium should evolve to the lowest-dissipation state/structure. In sharp contrast, our results obtained for a far-from-equilibrium system indicate that when multiple dissipative states are available, the non-minimally dissipative states can also be realized with finite probabilities. Interestingly, equations (1)–(3) asymptotically converge onto MEP when the dissipation gap $\Delta\varepsilon$ between the lowest and other possible dissipative structure(s) becomes very large (that is, when $\Delta\varepsilon\rightarrow\infty$). In this limit, self-assembly has no choice between similarly dissipative structures and chooses the least dissipative option with probability approaching unity (see point (3) above).

We emphasize that the comparison of the statistics we obtained with the MEP derived from thermodynamic considerations is a meaningful one. While the number of rotors in our system is small, the dissipation is due to the large number of molecules in the surrounding fluid. In other words, our system is macroscopic in a thermodynamic sense and the rotating particles play the role of moving boundaries in a macroscopic, continuum medium.

Regarding the functional form of equation (1), the presence of $\Delta\varepsilon$ in the denominator hints that dissipation in NE systems might play a role analogous to temperature in equilibrium systems. This would in turn imply that non-equilibrium trajectories visiting a steady-state are not determined by random collisions between the system and the bath but rather by the ability to dissipate energy to the surroundings to reach the ordered state. This line of reasoning also suggests that the observed structure probabilities reflect the phase-space dynamics of the system[2a,10] and the statistics of non-equilibrium paths leading to specific polymorphs.

Last but not least, we comment on why this work is aimed at a chemical rather than a physical audience. Historically, the development of equilibrium thermodynamics, from which chemistry has benefited so much, was crucially dependent on model systems, such as Lord Rumford's gun barrels (converting work into heat and leading to the first law of thermodynamics) or Watt's steam engines (inspiring Carnot's work and ultimately leading to the second law). Today, further progress in NE thermodynamics and its applications beyond the confines of near-equilibrium requires analogous test-beds that would inspire new theoretical approaches and experiments. We feel that chemists alone have the right palette of dynamic phenomena (for example, based on molecular switches, Stoddart's and Leigh's machines,[3d] or responsive nanocolloids[3a,c]) with which to synthesize dissipative structures, generalize results like ours to different length scales, and ultimately enable truly NE, life-like chemistries. In the meantime, the current work is significant in that it demonstrates that dissipation rates alone can dictate the outcomes of NE self-assembly, and that Nature does not always choose low-dissipation structures.

Methods

Simulation details: The system was approximated as a collection of n neutrally buoyant spheres of radius a rotating with constant angular velocity ω in a viscous fluid. The motion of the fluid outside the spheres was governed by the Navier–Stokes (NS) equations for an incompressible Newtonian fluid:

$\rho[\partial\vec{u}/\partial t+\vec{u}\cdot\nabla\vec{u}]=-\nabla p+\mu\nabla^2\vec{u}+f$ and $\nabla\cdot\vec{u}=0$

where $\vec{u}$ denotes the velocity vector, μ is the fluid viscosity, ρ is density, and f is the momentum source term. No-slip conditions were applied on the surfaces of the particles and NS equations were solved numerically on a cubical grid with periodic boundary conditions using the so-called force-coupling method (FCM), in which the solid spheres are approximated by locally distributed body forces acting on the fluid (see Ref. [7c] and the Supporting Information, Section S3 for further details).

The fluid motions induced by the rotating spheres gave rise to vortex–vortex forces. Introducing the stress tensor $\boldsymbol{\sigma}=-p\boldsymbol{\delta}+\mu\boldsymbol{\tau}$, where $\boldsymbol{\delta}$ is the unit tensor and $\boldsymbol{\tau}=[\nabla\vec{u}+(\nabla\vec{u})^t]$ is the viscous stress tensor, the force acting on sphere i can be expressed as $\vec{F}_D^{(i)}=\int_{S^{(i)}}\vec{n}\cdot dS^{(i)}$, where $\vec{n}$ is the unit normal directed outward from the particle, and integration is carried out over the surface of the sphere. Furthermore, all particles experienced magnetic forces produced by the rotating magnet and directed towards the axis of rotation of the magnet. As was shown previously,[7] these forces are well-approximated by the gradient of a quadratic "confining" magnetic potential, and can therefore be written as $\vec{F}_C=-\beta\vec{r}$, where $\vec{r}$ is the radial position vector. With these two forces, the dynamics of the particles in our system is described by, $m^{(i)}d\vec{V}^{(i)}/dt=\vec{F}_D^{(i)}+\vec{F}_C^{(i)}$, where $m^{(i)}=\frac{4}{3}\pi a^3\rho$ is the mass of particle i and $\vec{V}^{(i)}$ is its velocity. The energies are $K_{\{n,k\}}=\frac{m}{2}\sum_{i=1}^{n}V_i^2$, $U_{\{n,k\}}=\frac{\beta}{2}\sum_{i=1}^{n}r_i^2$, and $K^f_{\{n,k\}}=\frac{\rho}{2}\int_V u^2\,\mathrm{d}V$.

Viscous dissipation and entropy production: The expression for the viscous dissipation function Φ is given in the Supporting Information. The energy dissipation rate is related to the entropy production by $dS/dt=\int_V\sigma dV\approx 1/T\int_V\Phi dV=\varepsilon/T$; this equation provides a link to the Prigogine's MEP principle.

Received: February 17, 2013
Published online: July 14, 2013

Keywords: energy dissipation · entropy production · non-equilibrium · self-assembly

[1] *Directing Matter and Energy: Five Challenges for Science and for the Imagination*, Chap. 6, a report from the Basic Energy Sciences Advisory Committee, U.S. Department of Energy, **2009**. For electronic version, see http://science.energy.gov/~/media/bes/pdf/reports/files/gc_rpt.pdf.

[2] a) M. Fialkowski, K. J. M. Bishop, R. Klajn, S. K. Smoukov, C. J. Campbell, B. A. Grzybowski, *J. Phys. Chem. B* **2006**, *110*, 2482–2496; b) G. M. Whitesides, B. A. Grzybowski, *Science* **2002**, *295*, 2418–2421; c) M. F. Copeland, D. B. Weibel, *Soft Matter* **2009**, *5*, 1174–1187; d) M. K. Gardner, A. J. Hunt, H. V. Goodson, D. J. Odde, *Curr. Opin. Cell Biol.* **2008**, *20*, 64–70.

[3] a) S. C. Warren, O. Guney-Altay, B. A. Grzybowski, *J. Phys. Chem. Lett.* **2012**, *3*, 2103 – 2111; b) K. S. Toohey, N. R. Sottos, J. A. Lewis, J. S. Moore, S. R. White, *Nat. Mater.* **2007**, *6*, 581 – 585; c) S. Das, P. Ranjan, P. S. Maiti, G. Singh, G. Leitus, R. Klajn, *Adv. Mater.* **2013**, *25*, 422 – 426; d) B. Lewandowski et al., *Science* **2013**, *339*, 189 – 193; e) Y. H. Wei, S. B. Han, J. Kim, S. Soh, B. A. Grzybowski, *J. Am. Chem. Soc.* **2010**, *132*, 11018 – 11020; f) I. Lagzi, B. Kowalczyk, D. W. Wang, B. A. Grzybowski, *Angew. Chem.* **2010**, *122*, 8798 – 8801; *Angew. Chem. Int. Ed.* **2010**, *49*, 8616 – 8619; g) I. A. Chen, R. W. Roberts, J. W. Szostak, *Science* **2004**, *305*, 1474 – 1476.

[4] a) G. Nicolis, I. Prigogine, *Self-Organization in Nonequilibrium Systems: From DissipatiVe Structures to Order Through Fluctuations*, Wiley, Hoboken, **1977**; b) S. R. de Groot, P. Mazur, *Nonequilibrium thermodynamics*, Dover, **1984**; c) I. Prigogine, *Bull. Class Sci. Acad. R. Bel.* **1945**, *31*, 600 – 606.

[5] a) W. T. Grandy, *Entropy and the Time Evolution of Macroscopic Systems*, Oxford University Press, Oxford, **2008**; b) R. Landauer, *Phys. Rev. A* **1975**, *12*, 636 – 638.

[6] Minimization of entropy production and of energy dissipation has been invoked liberally in the context of photosynthesis (C. D. Andriesse, M. J. Hollestelle, *Biophys. Chem.* **2001**, *90*, 249 – 253), as a principle guiding evolution of organisms (B. Sabater, *Biosystems* **2006**, *83*, 10 – 17), as an ecological goal function (B. D. Fath, B. C. Patten, J. S. Choi, *J. Theor. Biol.* **2001**, *208*, 493 – 506), as a principle of optimal self-organization (D. Helbing, T. Vicsek, *New J. Phys.* **1999**, *1*, 13.1), and in many more situations where the very applicability of near-equilibrium concepts is, to put it mildly, questionable.

[7] a) B. A. Grzybowski, H. A. Stone, G. M. Whitesides, *Nature* **2000**, *405*, 1033 – 1036; b) B. A. Grzybowski, H. A. Stone, G. M. Whitesides, *Proc. Natl. Acad. Sci. USA* **2002**, *99*, 4147 – 4151; c) E. Climent, K. Yeo, M. R. Maxey, G. E. Karniadakis, *J. Flu. Eng. Trans. ASME* **2007**, *129*, 379 – 387.

[8] The Reynolds number for the rotating particles is defined as $\mathrm{Re} = \omega a^2/\nu$, where a is the particle radius and ν is kinematic viscosity of the medium. For Re of less than ca. 0.35, the particles do not rotate with constant ω or do not rotate at all when the fluid is too viscous. For Re of more than about 0.65, the assemblies that form sometimes disintegrate and then reassemble; these effects are due to experimental imperfections such as slight deviations in particle shape or "tilting" of the rotors with respect to the interface, and cannot be easily avoided even with extreme experimental care (for example, conducting the experiments in a closed chamber, on a vibration-control table, and so on).

[9] J. M. Bernal-García, A. Guzman-Lopez, A. Cabrates-Torres, V. Rico-Ramirez, G. A. Iglesias-Silva, *J. Chem. Eng. Data* **2008**, *53*, 1028 – 1031.

[10] a) A. N. Kolmogorov, *Dokl. Akad. Nauk SSSR* **1959**, *124*, 754 – 755; b) Y. G. Sinai, *Dokl. Akad. Nauk SSSR* **1959**, *124*, 768 – 771; c) V. Latora, M. Baranger, *Phys. Rev. Lett.* **1999**, *82*, 520 – 523; d) G. Nicolis, C. Nicolis, *J. Chem. Phys.* **1999**, *110*, 8889 – 8898; e) P. Gaspard, *Physica A* **2006**, *369*, 201 – 246.

